Rev.Adv.Mater.Sci. 18(2008) 439-443

IN-SITU OBSERVATION OF SOLIDIFICATION BEHAVIOUR FROM UNDERCOOLED α-Fe_2Si_5 MELT USING AN ELECTROMAGNETIC LEVITATOR

Kiyoshi Nozaki, Kosuke Nagashio and Kazuhiko Kuribayashi

Institute of Space and Astronautical Science (ISAS), Japan Aerospace Exploration Agency (JAXA), 3-1-1 Yoshinodai, Sagamihara, Kanagawa 229-8510, Japan

Received: March 29, 2008

Abstract. Fe_2Si_5 melts were deeply undercooled using an electromagnetic levitator and their growth velocity was measured by a high speed video camera in order to reveal the solidification behavior of intermetallic compounds. The growth morphology drastically changed depending on the undercooling, ΔT. The faceted planes were observed on the surface of the sample at $\Delta T \leq \sim 50$K. With increasing undercoolings, the morphology changed into typical facet dendrite. Especially at the high undercooling of $\Delta T \leq \sim 100$K, a dendrite of hexagonal symmetry clearly formed. The growth velocities were measured as a function of undercooling and compared with the classical dendritic growth theory. The interfacial kinetics is thought to be crucial for the solidification of Fe_2Si_5.

1. INTRODUCTION

Levitation techniques for the liquid droplet are important to study the solidification from undercooled melts because, by removing the crucible wall which is the preferential site of heterogeneous nucleation, they can positively control the undercooling as compared to other quenching techniques, [1]. In particular, an electromagnetic levitation (EML) is one of the suitable techniques for observing the solidification behavior of metallic systems *in situ* due to the free surface of the sample [2]. Recently, the EML has been applied to monatomic semiconductors. The substantial change of the macroscopic growth interface has been reported as a function of undercoolings [3,4], because a diamond structure has stronger anisotropy than the simple structures of metals.

Here, intermetallic compounds have stronger anisotropy and so their solidification behavior could be expected to differ from those of metals and monatomic semiconductors. However, to date, research understanding is insufficient for the solidification of intermetallic compounds from the undercooled melt. In this study, α-Fe_2Si_5 was selected because it possesses large crystallographic anisotropy as expected from *c*/*a*=1.91 [5]. In order to gain an insight into the mechanism of the solidification of the intermetallic compounds, the growth velocity and the growth interface morphology of α-Fe_2Si_5 were quantified as a function of undercoolings using a high-speed camera. Then, the growth kinetics were discussed in relation to the anisotropy of the crystal structure in order to provide some insights into the solidification mechanisms of other intermetallic compounds.

2. EXPERIMENTAL

Fe_2Si_5 ingot was prepared by arc melting Fe of 99.9% grade and Si of a semiconductor grade. Next, it was cut into small samples of ~0.6 g. The camber was evacuated to 10^{-4} Pa and backfilled with Ar gas of 5 N in purity. The sample was levi-

Corresponding author: Kiyoshi Nozaki, e-mail: kiyoshi.nozaki@isas.jaxa.jp

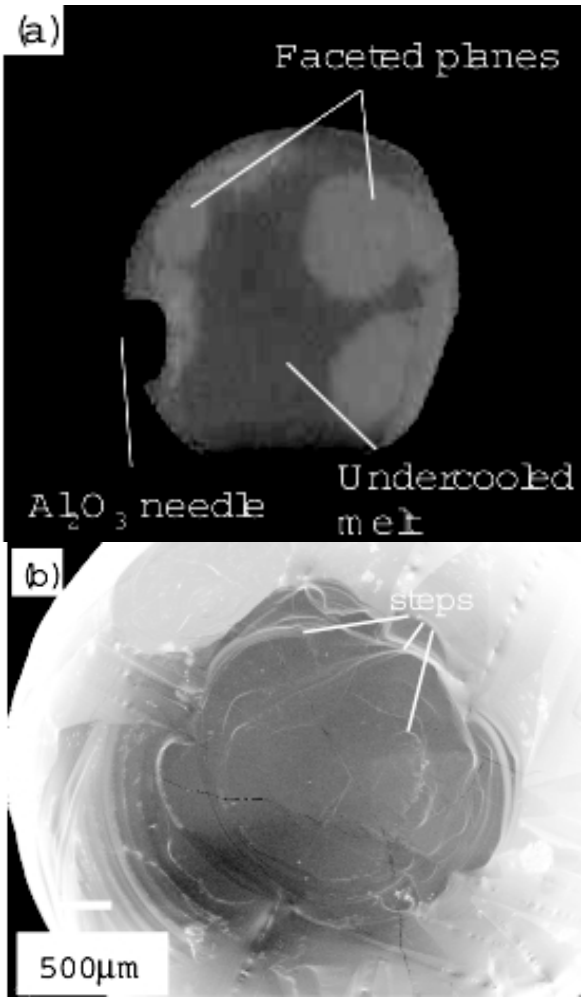

Fig.1. (a) High speed video image showing the facet planes of Fe_2Si_5 formed due to the forced nucleation by Al_2O_3 needle at ΔT = 20K. (b) SEM image of surface morphology of as-solidified Fe_2Si_5 at ΔT = 20K.

tated and melted by an electromagnetic coil in the camber. The molten droplet was cooled by flowing He gas of 5 N in purity to the bottom side of the sample. At the given undercooling, the sample was solidified by contact with an alumina trigger needle. The temperature of the sample surface was measured at 100 Hz by a two-color pyrometer with operating wavelengths of 900 and 1550 nm. Solidification behavior was monitored using a high-speed camera at 2 kHz; the growth velocities were calculated from the successive images obtained. The microstructures were investigated using an optical microscope and a scanning electron microscope (SEM).

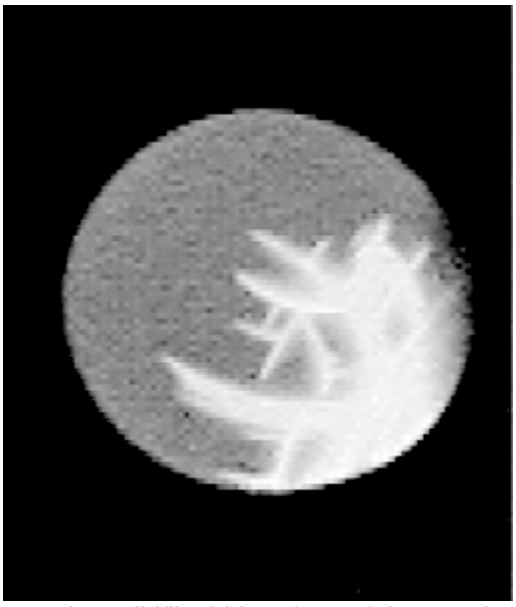

Fig. 2. The solid/liquid interface of the Fe_2Si_5 solidified by Al_2O_3 trigger needle at ΔT = 50K. Facet dendrites are clearly seen.

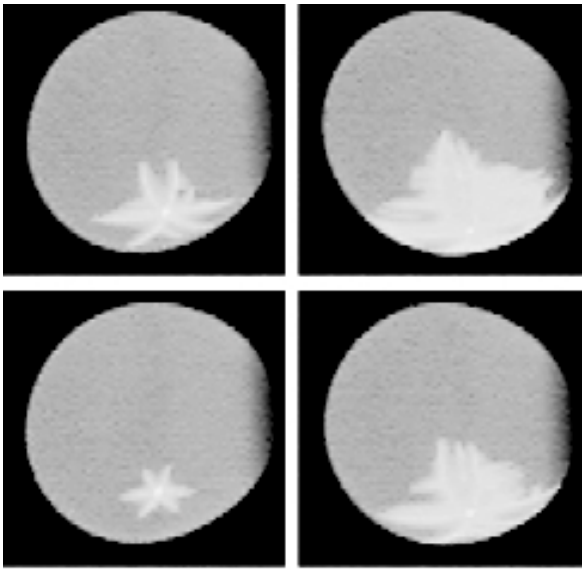

Fig. 3. Pictures of the Fe_2Si_5 solidification process observed by the high-speed camera at (a) t = 0.0025 s, (b) t = 5 ms, (c) t = 7.5 ms, and (d) t = 10 ms. Undercooling prior to spontaneous nucleation was 100K. A dendrite with hexagonal symmetry was clearly seen. At t = 7.5 ms, the high order arms appeared.

3. RESULTS AND DISCUSSION

Fig. 1a shows the solidification behavior at ΔT = 20K taken by the high-speed video. Many faceted

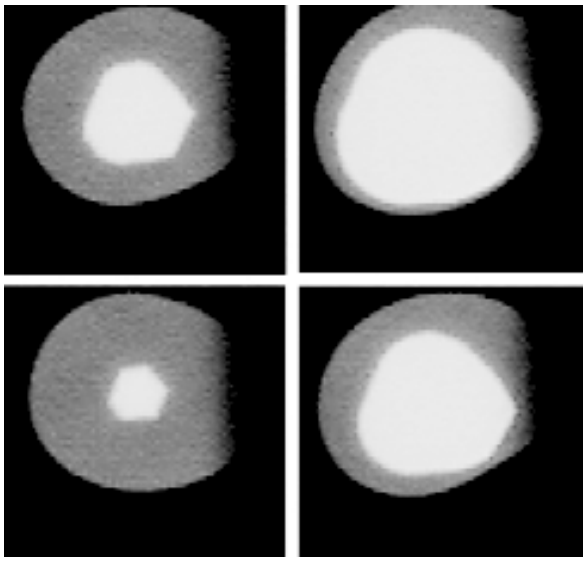

Fig. 4. Pictures of the Fe_2Si_5 solidification process observed by the high-speed video camera at (a) t = 5 ms, (b) t = 1 ms, (c) t = 15 ms, and (d) t = 20 ms. Undercooling prior to spontaneous nucleation was 150K. A hexagonal shape expanded on the surface.

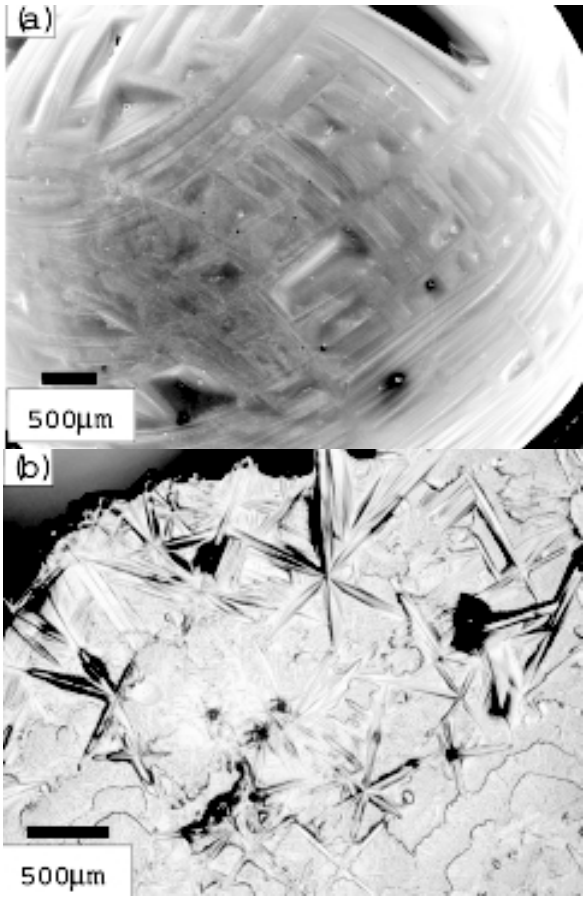

Fig. 5. (a) SEM image of surface morphology of the as-solidified sample at ΔT = 150K. The facet plane was not found on the surface. (b) The optical micrograph of the edge region of the sample quenched on a silicon plate. Many dendrites with the hexagonal symmetry were clearly detected.

planes were formed at the trigger point and floated on the droplet surface after detaching from the needle. This is the typical morphology at ΔT < 50K. Fig. 1b shows the SEM image of one facet plane observed on the sample solidified at ΔT = 20 K. The steps observed on the sample surface suggest that the solid/liquid interface would be stable even in the undercooled melt and that it would grow by the spiral growth mechanism. This kind of facet plane is seldom seen in the typical metallic system.

With increasing undercoolings, the morphology of the growth interface changed into a typical facet dendrite like semiconductors [3,4], as shown in Fig. 2. At higher undercoolings, a trigger needle was not used because the droplet was often triggered by the Al_2O_3 needle after spontaneous nucleation. Figs. 3 and 4 show the sequential images for the samples solidified spontaneously at ΔT = 100 and 150K, respectively. When nucleation accidentally occurred at the side proper for the camera, a dendrite of hexagonal symmetry was clearly detected at ΔT = 100K. On the other hand, the hexagonal shape was observed at ΔT = 150K. This would not be the facet plane which was observed at ΔT < 50K, because the facet plane was not found on the surface of the as-solidified sample, as shown in Fig. 5a. It can be expected that the secondary and higher-order arms, which usually developed at high undercoolings, macroscopically vary the interdendritic region and thereby yield the hexagonal shape. However, it was difficult to find dendrites with hexagonal symmetry on the surface of the as-solidified sample because they had been covered with the solidification of remaining melts at the plateau after recalescence. Therefore, the freezing of the dendritic microstructure was tried by dropping and quenching the molten droplet at around the melting point onto a silicon plate set below the levitation coil [6]. In this case, the facet dendrites with hexagonal symmetry were clearly observed near

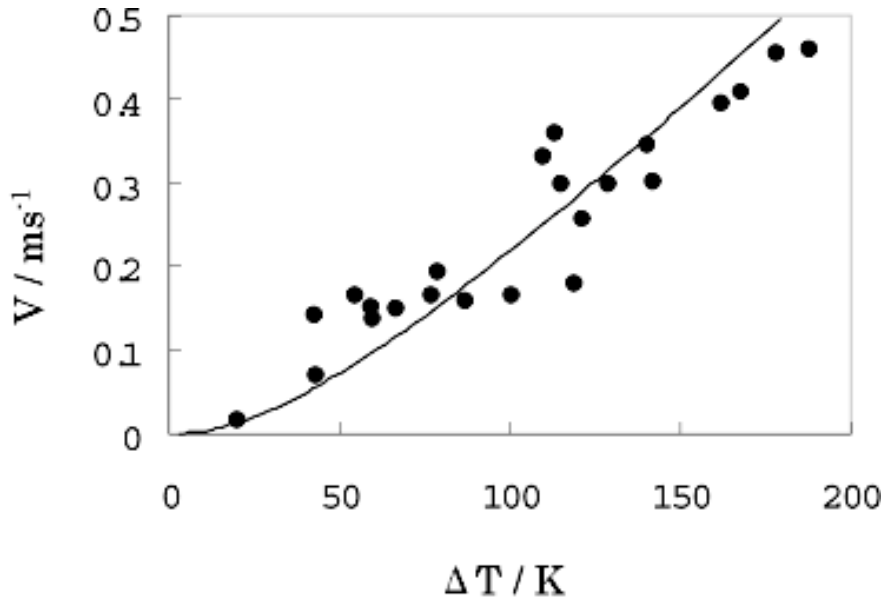

Fig. 6. Growth velocities measured by a high-speed video camera as a function of undercooling. The solid circles indicate experimental results measured by the high-speed video camera, while the solid line is the theoretical calculation using the dendrite growth model with m = 0.00052 $ms^{-1}K^{-1}$ [8].

the edge region of the quenched surface using the optical microscope, as shown in Fig. 5b.

In this study, the two-color pyrometer was used for the temperature measurement. From the two-color calibration, the emissivities of the solid and liquid were determined as 0.27 and 0.38, respectively. This difference in the emissivity led to the clear solid/liquid interface in the image even at low undercooling, as shown in Fig. 1, where the real temperature difference is very small [7]. Moreover, the large difference in emissivities of the solid and liquid suggests that the α-Fe_2Si_5 has some semiconducting properties although it has been recognized as a metallic compound, compared with β-$FeSi_2$.

The growth velocities of α-Fe_2Si_5 were measured as a function of undercoolings. Fig. 6 shows the relationship between growth velocity and bulk undercooling. The solid line in Fig. 6 indicates the theoretical curve calculated using the classical dendrite growth model with the kinetic undercooling [8]. In this model, the growth velocity and dendrite tip radius are independently determined by combining the diffusion solution by Ivantsov [9] and the marginal-stability analysis defined by Langer and Müller-Krumbhaar [10]. The physical properties used in the calculation were given elsewhere [11]. Only this system's kinetic coefficient, μ, has not yet been reported. Therefore, it was determined to be 0.0052 $ms^{-1}K^{-1}$ by fitting the theoretical calculation to the experimental results. Here, the kinetic coefficients of Si and FeSi have been reported as 0.4 $ms^{-1}K^{-1}$ [12] and 0.014 $ms^{-1}K^{-1}$ [13], respectively. The comparison of the kinetic coefficients suggests that the interfacial kinetic coefficient would be crucially dependent on the crystal structure of the materials and that the incorporation of atoms at the growth interface is the rate-limiting factor for the solidification of α-Fe_2Si_5 due to the highly complex structure.

4. CONCLUSIONS

The growth interface of α-Fe_2Si_5 was monitored by a high-speed video camera and the growth velocities of undercooled melt were measured from the successive images in order to elucidate the solidification behavior of the intermetallic compounds with high crystal structure anisotropy. With increasing undercoolings, the morphology changed from facet planes to typical facet dendrites with hexagonal symmetry. The growth velocities measured

were much smaller than those of typical metallic and semiconductor materials with simpler crystal structure. These results suggest that the growth of α-Fe_2Si_5 is controlled by the interfacial kinetics.

REFERENCES

[1] G.J. Abbaschian and M.C. Flemings // *Metall. Trans. A* **14A** (1983) 1147.
[2] D. Li, K. Eckler and D.M. Herlach // *J.Cryst. Growth* **160** (1996) 59.
[3] T. Aoyama, Y. Takamura and K. Kuribayashi // *Metall. Mater. Trans. A* **30A** (1999)1333.
[4] T. Aoyama and K. Kuribayashi // *Acta Mater.* **48** (2000) 3739.
[5] F.A. Sidorenko, P.V. Gel'd and L.B. Dubrovskaya // *Fiz.Met.Metalloved.* **8** (1959) 735.
[6] K. Nagashio, H. Murata and K. Kuribayashi // *Acta Mater.* **52** (2004) 5295.
[7] T. Aoyama, Y. Takamura and K. Kuribayashi // *Jpn.J.Appl.Phys.* **37** (1998) L687.
[8] J. Lipton, W. Kurz and R. Trivedi // *Acta Metall.* **35** (1987) 957.
[9] G. P. Ivantsov // *Dokl. Akad. Nauk. SSSR.* **58** (1947) 567.
[10] J. S. Langer and H. Müller-Krumbhaar // *Acta Metall.* **26** (1978) 1681.
[11] K. Yamamoto, S. Ozawa, Y. Nakamura, S. Sugiyama, I. Jimbo and K. Kuribayashi // *Microgravity sci. technol.* **XVI-I** (2005) 136.
[12] K. Nagashio, H. Okamoto, K. Kuribayashi and I. Jimbo // *Metall. Mater. Trans. A* **36A** (2005) 3407.
[13] M. Barth, B. Wei and D.M. Herlach // *Phys. Rev. B* **51** (1995) 3422.